Sustainable Chemical Engineering
http://ojs.wiserpub.com/index.php/SCE/

UNIVERSAL WISER PUBLISHER

Research Article

Air Quality Assessment Based on a Smart Locally CO_2 Monitoring System with Validation by a Reference Instrument

Jacob Mbarndouka Taamté[1*], Vitrice Ruben Folifack Signing[1], Modibo Oumar Bobbo[1], Kountchou Noubé Michaux[1], Yerima Abba Hamadou[1], Saïdou[1,2]

[1]Research Centre for Nuclear Science and Technology, Institute of Geological and Mining Research, Yaounde, Cameroon
[2]Nuclear Physics Laboratory, Faculty of Science, University of Yaounde, Yaounde, Cameroon
Email: mtjfirst@yahoo.fr

Received: 15 January 2024; **Revised:** 11 March 2024; **Accepted:** 12 March 2024

Abstract: This article deals with the development and implementation of a low-cost smart air quality monitoring device. The study aims to develop a simple, efficient, and cheap device for real-time monitoring of Carbon dioxide (CO_2) concentration and atmospheric parameters such as temperature (T) and relative humidity (RH). The realized device consists of sensors, a data storage system, a programmable card, and wireless modules for Internet of Things (IoT). It is designed for indoor and outdoor air quality monitoring. Wireless communication between the device and the control PC is ensured by the ZigBee protocol. The MH-Z14A sensor was calibrated according to the manufacturer's recommendations and then experimentally in the laboratory. A calculation of the CO_2 regression line for the devices using the least squares method gave $R^2 = 0.6889$. The slope test using the Student method at a significant coefficient of 1% threshold and 19 degrees of freedom gave $t(1\%; 19) = 2.539$. This illustrates that the result obtained by the realized device has less than a 1% chance of being obtained at random. An investigation was carried out to assess air quality because following the proliferation of pollutants, the normal concentration of atmospheric CO_2 (400 ppm) has considerably changed. Thus, the data processed are outdoor concentrations collected in November 2022 in some localities of the Adamawa Region, Cameroon. The average values of CO_2 concentration measured in four subdivisions are 497.30 ± 11.32 ppm in Ngaoundéré 1, 481.83 ± 14.90 ppm in Ngaoundéré 2, 568.63 ± 25.03 ppm in Martap and, 624.14 ± 3.96 ppm in Minim. Martap and Minim are among the most important bauxite deposits in the world. These CO_2 values higher than the normal atmospheric concentration indicate a moderate Air Quality Index (AQI) in these cities during the measurement period. The designed device is inexpensive, reliable, and appropriate for air quality monitoring.

***Keywords*:** air quality monitoring, carbon dioxide, microcontroller, low-cost sensors, IoT device, ZigBee protocol

1. Introduction

Air pollution is the greatest environmental and public health challenge in the world today[1]. One of the main causes of global warming is the emission of CO_2 into the atmosphere[2]. Currently, the decline in air quality in large cities continues to increase due to industrial growth, road traffic, and population growth[3]. Living beings transform oxygen into CO_2 through respiration, while plants use CO_2 for photosynthesis and transform it into organic carbon compounds (sugars, cellulose, etc.) and dioxygen (O_2), commonly known as oxygen[4]. The importance attributed to CO_2 comes from the

DOI: https://doi.org/10.37256/sce.5120244286

rapid increase in CO_2 concentration in the atmosphere as a result of increasing fossil fuel consumption and a significant reduction in forest cover on a global scale[5]. On a planetary level, CO_2 is part of human-caused pollutant emissions; its emissions have two origins: natural and anthropogenic[6]. The current average rate of CO_2 concentration in the air (in ppm) oscillates around 0.038% (0.1% = 1,000 ppm) with some day-night, seasonal variations, and pollution peaks[7]. CO_2 is a greenhouse gas and contributes greatly to the increases in the earth's temperature by intercepting the infrared rays reflected from the earth's surface[8]. Global warming promotes the atmospheric accumulation of water vapor, the atmosphere becomes humid and traps more and more heat[9-11]. From a health perspective, CO_2 has a very high dissolving capacity in the mucous membranes of the human body and causes numerous reactions as soon as its concentration in the inspired air increases. For concentrations close to 0.1%, CO_2 alters the respiratory rate of people who suffer from respiratory insufficiency. Levels above 1,000 ppm in a closed environment can lead to asthma attacks[12,13].

Due to the danger of CO_2, researchers developed a low-cost, pocket-sized CO_2 device with flexible applications that yields benefits for students and schools[14,15]. The advantage of this device is that it is low-cost, but does not have an IoT module and is not included in the scope of delivery so that it can be used on-site. Gonçalo Marques et al. realized an IoT-based CO_2 monitoring system to assess indoor air quality assessment[16,17]. They have developed a low-cost device that uses a Wi-Fi module for data transmission to the Cloud. This means that we will need a permanent internet connection and in the long term, this will become expensive. In addition, the device is not in the box and its functionality is only limited to indoor measurement. Dari et al. designed and built a hazardous gas monitoring device (CO, CO_2, CH_4) on cigarette smoke in an enclosed space based on Arduino Uno and GSM SIM 900 A[18]. They have always offered a low-cost device with IoT functionality, but except that they use MQ sensors which are metal oxide semiconductor sensors that are very unstable and difficult to calibrate[18]. Several works on CO_2 are being carried out around the world. Some realize the device and use it to measure CO_2 while others capture CO_2[19-21].

According to the Mauna Loa Observatory (MLO), atmospheric CO_2 is higher today than at any time in the past 200,000 years of human history[22]. In fact, studies of past CO_2 levels have accumulated evidence that CO_2 levels have been below 400 ppm (parts per million) for the past 23 million years[23]. This makes CO_2 records today the highest in human history. Statistics show that we now consider air with 420 ppm of CO_2 and 21 percent of oxygen to be fresh. However, the norm used to be no more than 350 ppm[24,25]. With this rise of almost 100 points in 50 years, it becomes clear there is a need for the constant monitoring of indoor and outdoor levels of CO_2[26-28].

CO_2 monitors in general are decision-making tools regarding air pollution. It is in this context that an intelligent, simple, effective and inexpensive device is produced in this article as an appropriate solution for knowing CO_2 concentrations in real-time. The proposed system is manufactured locally based on the microcontroller card, XBee S2C modules, temperature, relative humidity and CO_2 sensors whose reliability has been confirmed in[29-34]. The final device was packaged in the box to facilitate its deployment in the field by using rechargeable batteries. Methods such as the least squares method to determine the correlation coefficient $R^2 = 0.6889$ and the Student method to test the slope of the regression line of the concentrations of CO_2 were applied during the calibration process of the realized device, in order to note that the result of the realized device has less than 1% chance of being obtained at random. Data were collected in November 2022 in the city of Ngaoundéré and two localities in the bauxite zones of Minim and Martap in the Adamawa region of Cameroon. Real-time data acquisition was supervised and remotely monitored via the IoT functionality of the device. The collected data was stored in a digital card before being analyzed to assess air quality based on the obtained CO_2 levels. These results were also compared to the international standards of the Mauna Loa Observatory (MLO)-USA and the National Agency for Food, Environmental and Occupational Health Safety (ANSES)-French[35-38].

2. Material and methods

2.1 *Study areas*

The CO_2 measurements in this article were carried out in two divisions of the Adamawa region, namely three districts in the Vina division and one district in the Djérem division. Figure 1 shows the location of the Adamawa region and the subdivisions where the measurements were taken.

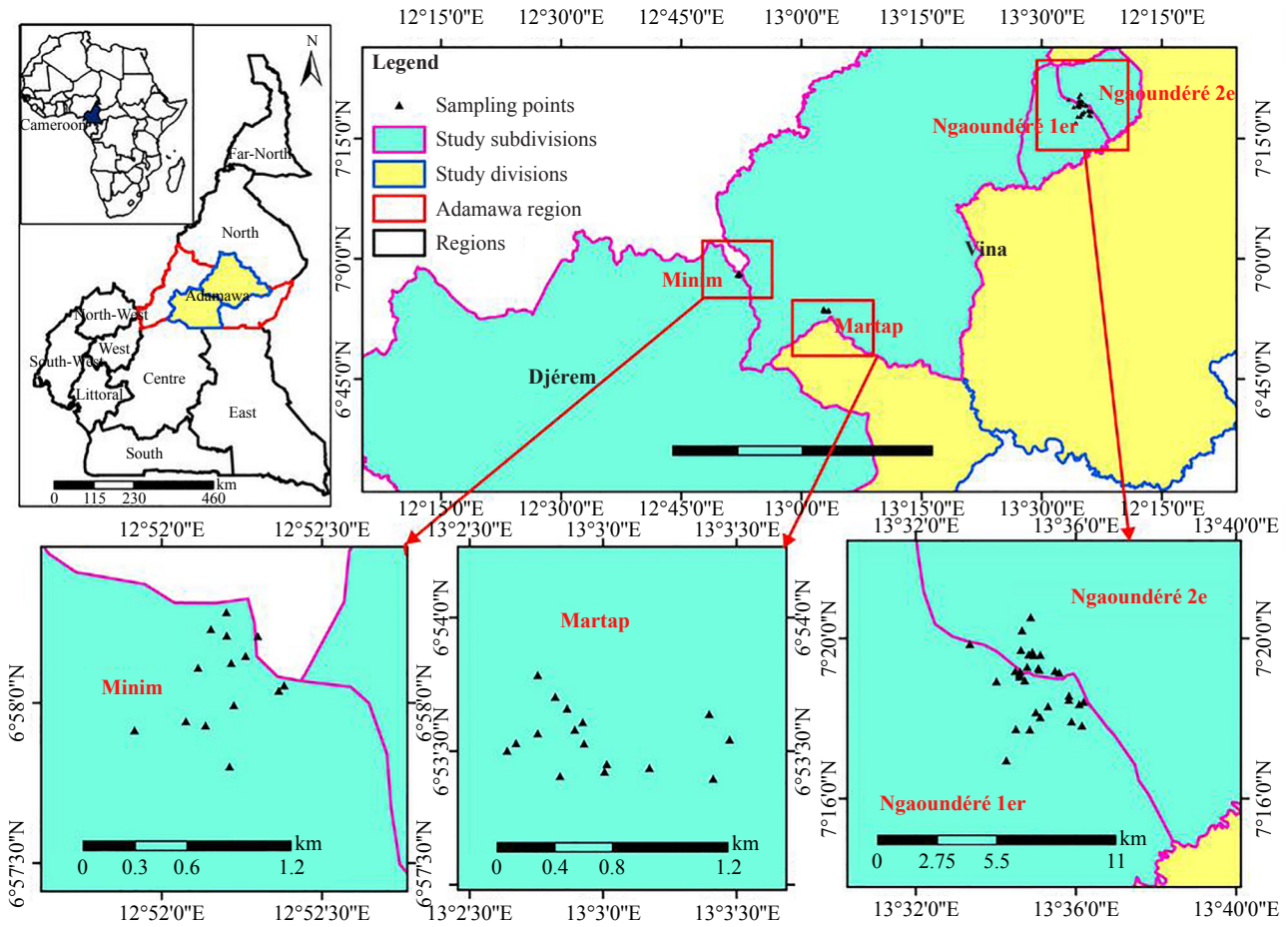

Figure 1. Location of CO_2 measurement points

Table 1. Geographical coordinates of the measurement points taken in Ngaoundéré 1 and 2

Measuring point of Ngaoundéré 1	latitude N	longitude E	Measuring point of Ngaoundéré 1/Ngaoundéré 2	latitude N	longitude E
N1	7°17'49,38"	13°36'8,82"	N17	7°19'35,23"	13°35'6,56"
N2	7°17'49,39"	13°36'8,84"	N18	7°18'27,90"	13°35'49,29"
N3	7°16'57,13"	13°34'15,55"	N19	7°18'55,63"	13°35'0,65"
N4	7°17'44,10"	13°34'29,87"	N20	7°19'11,17"	13°34'28,80"
N5	7°17'43,46"	13°34'50,70"	K1	7°19'8,64"	13°35'34,96"
N6	7°18'1,95"	13°35'6,32"	K2	7°19'11,21"	13°35'28,46"
N7	7°18'9,26,32"	13°34'59,81"	K3	7°19'13,11"	13°35'5,02"
N8	7°18'18,19"	13°35'18,04"	K4	7°19'15,34"	13°35'3,53"
N9	7°17'55,46"	13°35'53,19"	K5	7°19'17,22"	13°34'46,80"

Table 1. (cont.)

Measuring point of Ngaoundéré 1	latitude N	longitude E	Measuring point of Ngaoundéré 1/Ngaoundéré 2	latitude N	longitude E
N10	7°18'24,85"	13°36'11,42"	K6	7°19'39,46"	13°34'54,63"
N11	7°18'21,50"	13°36'4,91"	K7	7°19'34,98"	13°34'57,04"
N12	7°18'34,16"	13°35'49,34"	K8	7°19'36,01"	13°34'49,23"
N13	7°19'10,28"	13°34'36,30"	K9	7°19'42,51"	13°34'37,35"
N14	7°19'6,86"	13°34'35,14"	K10	7°20'12,01"	13°34'38,98"
N15	7°19'2,91"	13°34'35,35"	K11	7°20'31,77"	13°34'52,07"
N16	7°18'56,94"	13°34'43,21"	K12	7°19'51,46"	13°33'20,88"

Table 2. Geographical coordinates of measurement points taken at Martap and Minim

Measuring point of Martap	latitude N	longitude E	Measuring point of Martap/Minim	latitude N	longitude E
M1	6°53'36,50"	13°2'55,40"	M16	6°53'32,60"	13°3'28,40"
M2	6°53'39,60"	13°2'51,90"	L1	6°57'59,60"	12°52'13,50"
M3	6°53'34,80"	13°2'53,60"	L2	6°58'7,50"	12°52'13,00"
M4	6°53'24,4"	13°2'50,3"	L3	6°58'6,60"	12°52'6,80"
M5	6°53'34,00"	13°2'45,30"	L4	6°58'17,00"	12°52'12,10"
M6	6°53'30,10"	13°2'38,40"	L5	6°58'3,30"	12°52'22,90"
M7	6°53'31,80"	13°2'40,40"	L6	6°58'2,30"	12°52'21,90"
M8	6°53'47,10"	13°2'45,30"	L7	6°58'9,30"	12°52'66,90"
M9	6°53'42,20"	13°2'49,20"	L8	6°58'6,60"	12°52'44,18"
M10	6°53'31,70"	13°2'55,70"	L9	6°58'12,60"	12°52'12,16"
M11	6°53'27,10"	13°3'00,80"	L10	6°58'50,60"	12°52'4,50"
M12	6°53'25,40"	13°3'00,30"	L11	6°58'12,50"	12°52'18,00"
M13	6°53'26,20"	13°3'10,40"	L12	6°58'60,1"	12°52'12,7"
M14	6°53'23,80"	13°3'24,70"	L13	6°58'70,7"	12°52'9,20"
M15	6°53'38,30"	13°3'23,80"	L14	6°58'80,8"	12°52'15,7"

The main objective of this article is to realize a low-cost atmospheric CO_2 rate monitoring device. However, it is

important to geolocate the study area to facilitate the identification and visualization of sampling points. Figure 1 shows the state of this study area and the sampling points are represented by the black triangles on the map. For this study, 62 measurement points were carried out, namely 20 points (from N1 to N20) in the district of Ngaoundéré 1, 12 (from K1 to K12) in the district of Ngaoundéré 2, 16 (from M1 to M16) in the district of Martap and 14 (from L1 to L14) in Minim town which belongs to the district of Tibati. Tables 1 and 2 show the geographical coordinates of the different measurement points carried out in the four study cities.

2.2 *Design of real-time CO_2 monitoring device*

The developed real-time CO_2 device is based on an Arduino board (data processing and analysis unit), XBee wireless, temperature, relative humidity, and CO_2 sensors. The final prototype is powered by three rechargeable batteries of 3.7 V each, for autonomous measurements. The main measured molecule is carbon dioxide, which is detected by the MH-Z14A sensor. Data transmission between the device and the remote PC is provided by the XBee radio frequency and the IoT module. A schematic diagram of the CO_2 device and the used monitoring system is shown in Figure 2 and Figure 3, respectively.

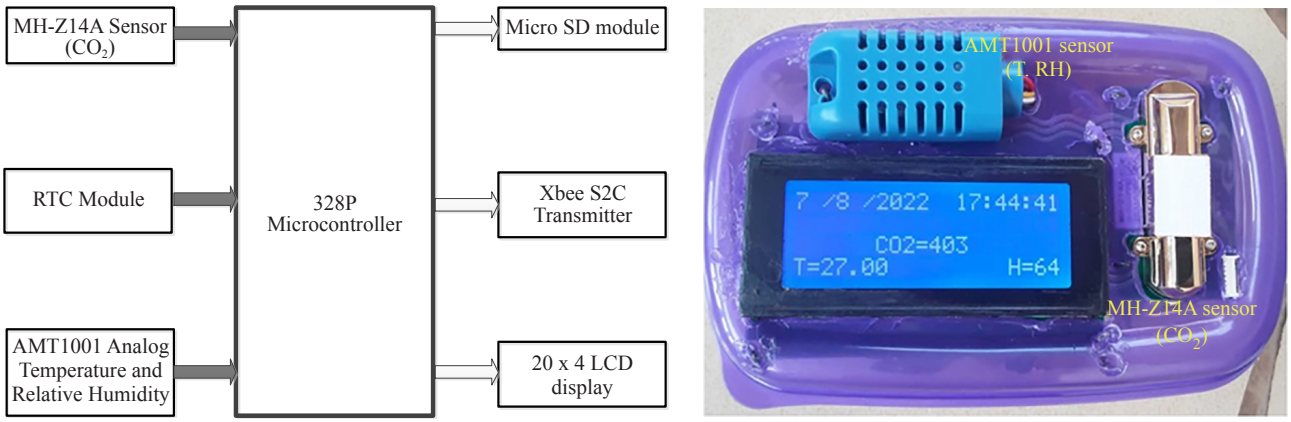

Figure 2. Schematic diagram of the realized CO_2 monitoring device

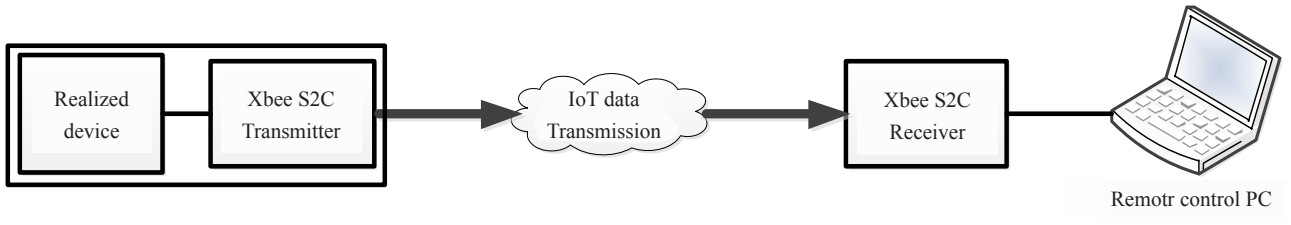

Figure 3. Schematic diagram in IoT operation of the CO_2 monitoring system

The MH-Z14A NDIR infrared gas module is a common small sensor that uses the non-dispersive infrared (NDIR) principle to detect the existence of CO_2 in the air, with good selectivity, non-oxygen dependent and long life. Integrated temperature compensation, digital output and PWM output.

The AMT1001/AM1001 is a moisture-resistant temperature and humidity sensor, a single wet sensor that sends signals via an analog voltage output. This module features high accuracy, high reliability, consistency, and temperature compensation to ensure long-term stability, ease of use and low price.

The XBee S2C modules use the ZigBee radio communication protocol based on the IEEE 802.15.4 standard

with an operating frequency of 2.4 GHz. They facilitate remote data transmission, between an electronic device and a computer through two XBee transmitter and receiver modules and the XCTU application previously installed on the PC.

Table 3. Technical characteristics of the used electronic sensors

Types of sensors	Measured gas	Detection capability	Sensor accuracy	Operating energy	Response time
MH-Z14A	CO_2	0~10,000 ppm	± 50 ppm ± 5%	4~6V DC	< 30s
AMT1001/AM1001	Temperature	0~50 °C	± 2 °C	4~5.5V DC	≈ 10s
	Relative Humidity	20~90%RH	± 5%RH		

2.3 *Sensors calibration and device operation algorithm*

Detection and measurement sensors require calibration and configuration processes before use. The sensors used in this work are experimentally calibrated in the laboratory according to the manufacturer's instructions. For the MH-Z14A sensor, we performed zero point calibration and this module has three methods for its zero point calibration namely manual method, command sending method and self-calibration[39,40]. Its zero point is set at a CO_2 concentration of 400 ppm. The manual method was to connect the HD pin of the sensor to a low level (0 V) for a few seconds (10 seconds) while ensuring that the sensor was stable for half an hour of operation in an ambient environment of 400 ppm. Calibration of the MH-Z14A sensor using the send command method was not performed due to the lack of a serial port (URAT). Self-calibration, on the other hand, was performed by running the module in the laboratory every 24 hours for a week. During these running times, the module intelligently judges the zero point and automatically performs a zero calibration each time the power is turned on.

The final calibration of the MH-Z14A and AMT1001 sensors, whose technical specifications are shown in Table 3, was carried out in the laboratory in the presence of a reference device. The two devices shown and referenced in Figure 4 were used in the same location and under the same atmospheric conditions for three weeks to measure temperature, relative humidity and CO_2 concentration.

Figure 4. Calibration process

The results obtained are shown in Figure 5, (a) for the temperatures of the two devices, (b) for humidities and (c) for CO_2 concentrations.

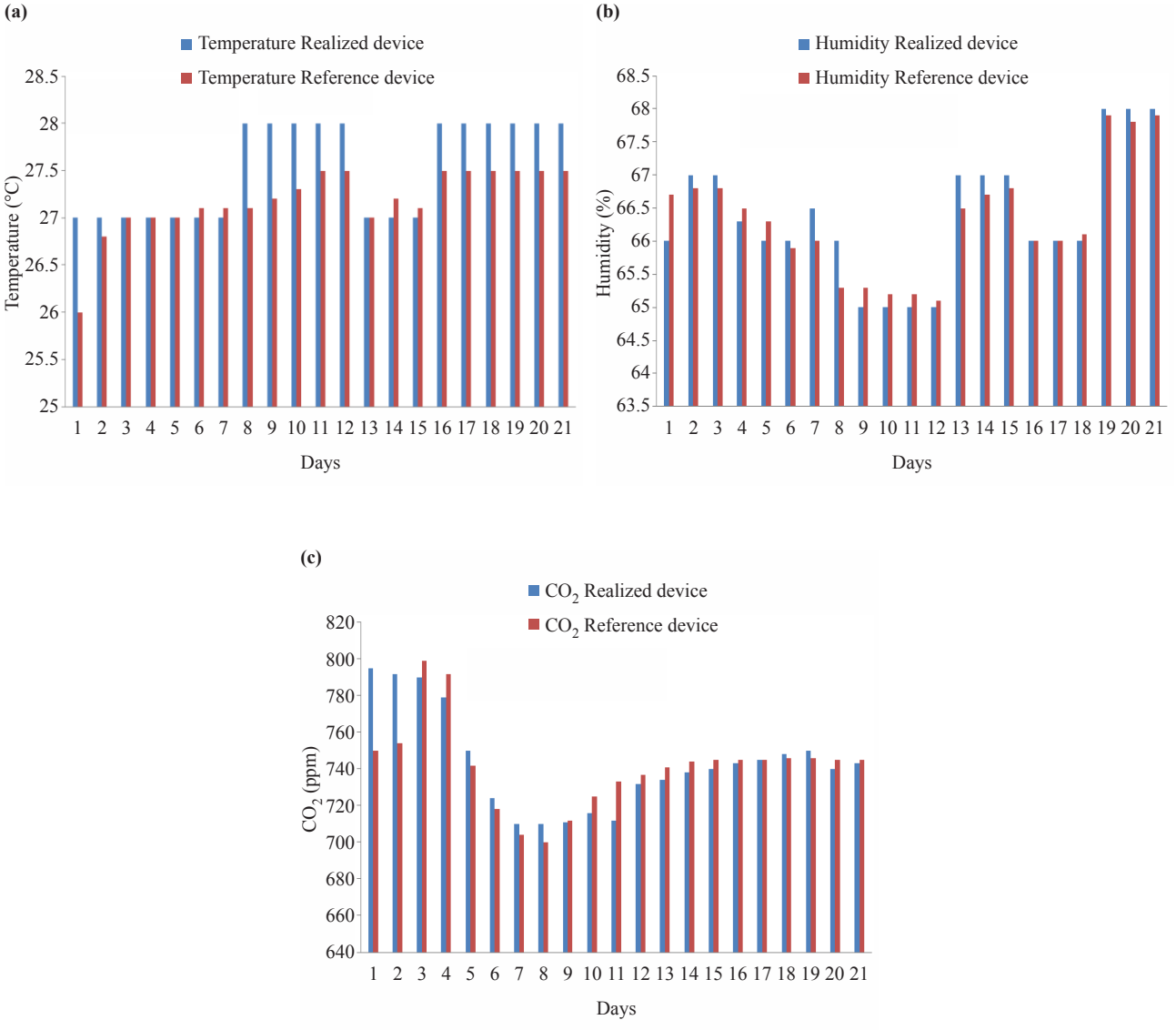

Figure 5. Test measurements performed for the realized device calibration process

The temperatures and relative humidities measured by the two devices are similar at some points and show small differences at other points. These results give mean values of 27.52 ± 0.51 °C and 66.37 ± 0.96% for the realized device and 27.17 ± 0.36 °C and 66.32 ± 0.86% for the reference device. These values are almost identical. With the CO_2 sensor, the concentrations given by the realized device remained higher than those of the reference device throughout the first week of measurement (Figure 5 (c)) and from the second and third week of measurement the concentrations delivered by the two devices remained almost identical. The average values obtained are then 742.95 ± 26.67 ppm for the realized device and 739.42 ± 19.80 ppm for the reference device.

An in-depth statistical study of the results obtained is necessary to better assess the reliability of the realized device. Therefore, it is important to calculate the equation of the regression line $y = ax + b$ of the CO_2 concentrations of the two devices by using the least squares method and perform the slope test using the Student method[41,42]. Let x be

the CO_2 concentrations from the reference device and y those of the realized device. The values of the slope a and the ordinate at the origin b are obtained from the following equations (1) and (2):

$$a = \frac{\mathrm{cov}(x, y)}{\sigma_x^2} = 1.12 \tag{1}$$

$$b = \bar{y} - a\bar{x} = -85.2 \tag{2}$$

With cov(x, y) = 440.72 the covariance of x and y, σ_x = 19.80 and σ_y = 26.68 the standard deviations of x and y, $\bar{x}$ = 739.42 and $\bar{y}$ = 742.95 the mean values of x and y. The equation of the regression line of the CO_2 concentrations of the two devices is then obtained:

$$y = ax + b = 1.12x - 85.2 \tag{3}$$

We deduce from the cov(x, y) and the standard deviations of x and y, the existence of a very strong positive linear correlation between the two variables:

$$R = \frac{\mathrm{cov}(x, y)}{\sigma_x \sigma_y} = 0.83$$

$$R^2 = 0.6889 \tag{4}$$

Verification of the results of equations (3) and (4) obtained by the least squares method was carried out in Microsoft Excel as presented in Figure 6. In both methods, we almost obtained the same regression line y = 1.12x – 85.6, with R^2 = 0.6889 ≈ 0.76.

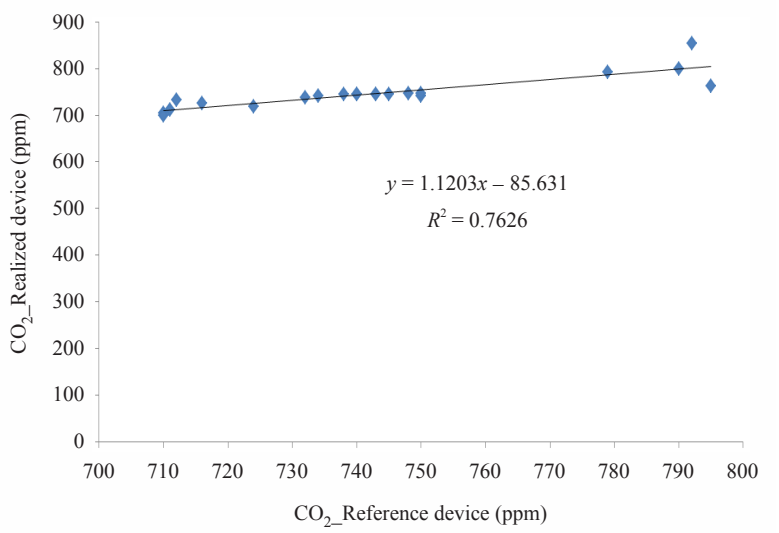

Figure 6. Equation of the regression line and correlation coefficient obtained with Microsoft Excel

To perform the test of the slope using Student's method, it is necessary to calculate the coefficient t so that:

$$t_a = \frac{a}{\sigma_a} = 6.22 \tag{5}$$

With

$$\sigma_a = \frac{\sigma_r}{\sqrt{\sum_i (x_i - \bar{x})^2}} = 0.18 \tag{6}$$

$$\sigma_r = \sqrt{\frac{\sum_i r_i^2}{n-2}} = 15.67 \tag{7}$$

With r the residue such that $r = y_i - \hat{y} = e$; the error between the observed value y_i and the estimated value $\hat{y}$. σ_r is the standard deviation of the residuals, σ_a the standard deviation of the slope a of the regression line, n the number of observations i.e., the measurements taken and $(n - 2)$ the degree of freedom with 2 number of independent variables x and y. It is essential to make assumptions for the significance test of the regression coefficients. Thus, we first pose $H_0 : \beta = 0$, when the concentration x of the reference device has no influence on the concentration y of the realized device and secondly $H_1 : \beta \neq 0$, when the concentration x has an influence on the concentration y. By choosing a significant coefficient at a 1% threshold with 21 CO_2 concentration measurements carried out, i.e. 19 degrees of freedom, the reading of the Student's law table of $t_{(1\%;\ 19)}$[43,44] gives:

$$t_{(1\%;\ 19)} = 2.539 \tag{8}$$

As $t_a > t_{(1\%;\ 19)}$, then the hypothesis H_0 is rejected therefore there is a significant linear relationship at the 1% risk between the CO_2 concentrations measured by the two devices. In other words, the result obtained by the produced device has less than 1% chance of being obtained at random.

For the use of sensors in the measurement of air pollutants, computer programming and experimental work were performed on a computer with specifications Intel (R) Core (TM)i7-4600M, 2 Duo CPU 2.9 × 2 GHz, 8 GB RAM with Windows 10-64 bit professional as the operating system. The simulation environment is the Arduino IDE, whose operating algorithm is programmed for the monitoring device. The complete operation algorithm of the realized device is described in detail as Appendix.

2.4 *Threshold and effects of CO_2 on metabolism*

At low concentrations, CO_2 is harmless to human health, but long-term exposure can cause headaches. CO_2 is also a good marker for measuring indoor air renewal. The normal indoor concentration varies between 400 and 1,000 ppm. Above this threshold, the negative effects on human health can increase and can lead to death at concentrations above 40,000 ppm[45,46]. This is described by ANSES[37] describes in Table 4 below:

Table 4. Threshold and effects of CO_2 on metabolism[37,47]

N°	CO_2 concentrations (ppm)	Symptoms
1	From 250 to 350	Background outside air level (normal)
2	From 350 to 1,000	Typical air level found in occupied spaces with good air exchange
3	From 1,000 to 2,000	First effects: Complaints of drowsiness and bad air
4	From 2,000 to 5,000	Headaches, poor concentration, loss of attention, increased heart rate and mild nausea
5	5,000	Unusual air conditions/presence of other gases. Toxicity or oxygen deprivation that may occur. (Permissible workplace exposure limit)
6	40,000	Immediately harmful level due to oxygen deprivation
7	70,000	Suffocation even in the presence of oxygen
8	100,000	Unconsciousness, coma or asphysis within minutes
9	250,000 and +	Death

3. Results and discussion

3.1 *Atmospheric CO_2 measurement*

Figures 7, 8 and 9 show the CO_2 concentrations, temperature, and humidity obtained in the four cities of the study area.

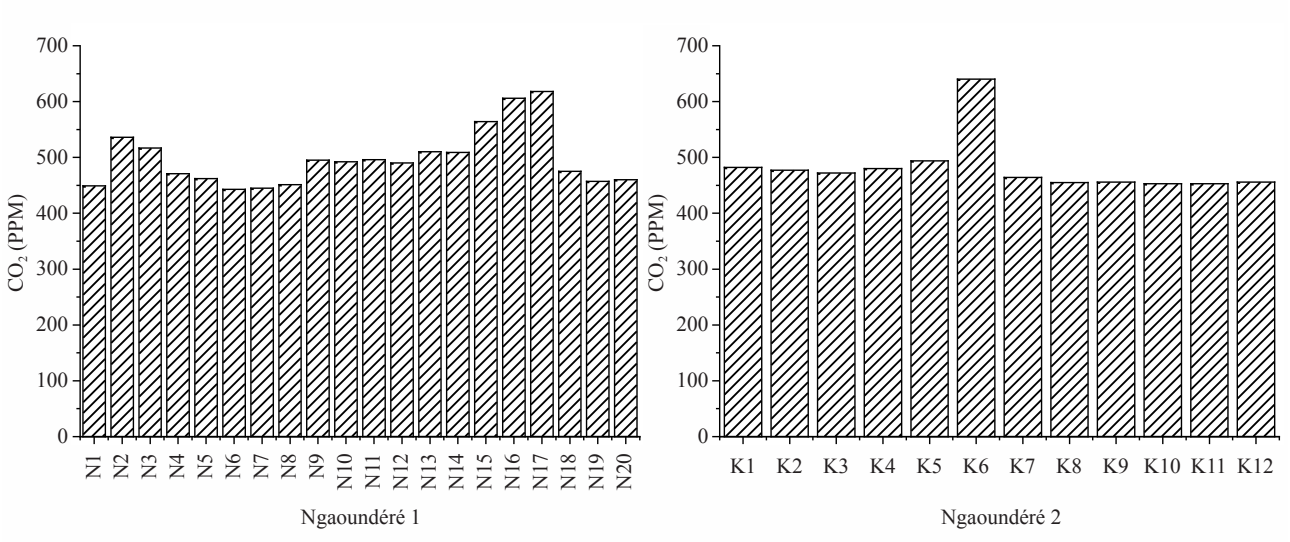

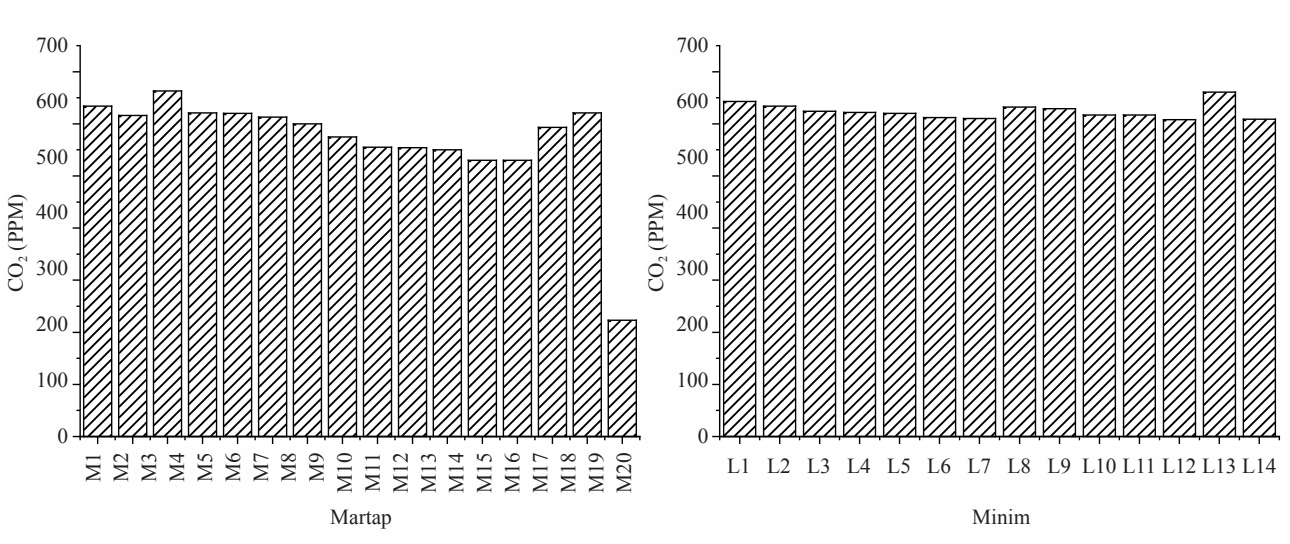

Figure 7. CO_2 concentrations obtained in the measurement localities

CO_2 concentrations in Ngaoundéré 1 district are between 450 and 650 ppm, in Ngaoundéré 2 district almost all values are below 500 ppm, except of a single value which represents a concentration pick of CO_2 around 650 ppm. In the Martap and Minim districts, most CO_2 concentrations are high, around 600 to less than 700 ppm. A low CO_2 concentration of around 200 ppm was obtained in the city of Martap. The measuring device must certainly be influenced by errors at this measuring point. The obtained values in these four localities are higher than the normal concentration of atmospheric CO_2 which is 400 ppm[48,49]. This may be because the measurements were carried out in public places, namely markets, city centers, schools, family homes, and hospitals where there are a large number of people who produce CO_2 through the mechanism of respiration. It was important to carry out the measurements in these environments because the primary objective of the application of this work is the protection of people.

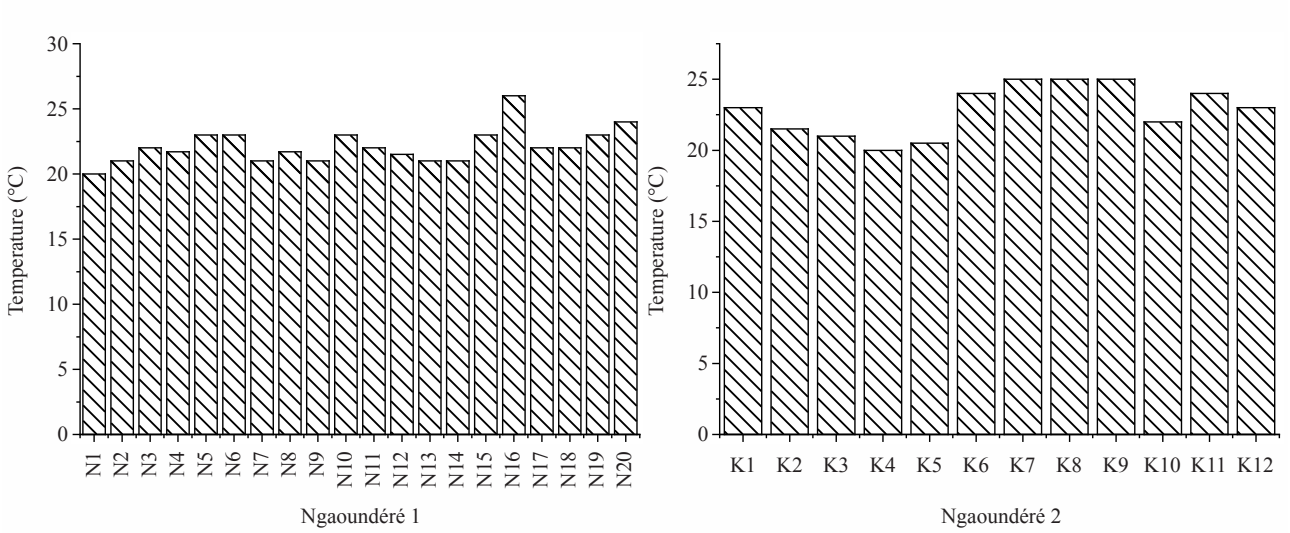

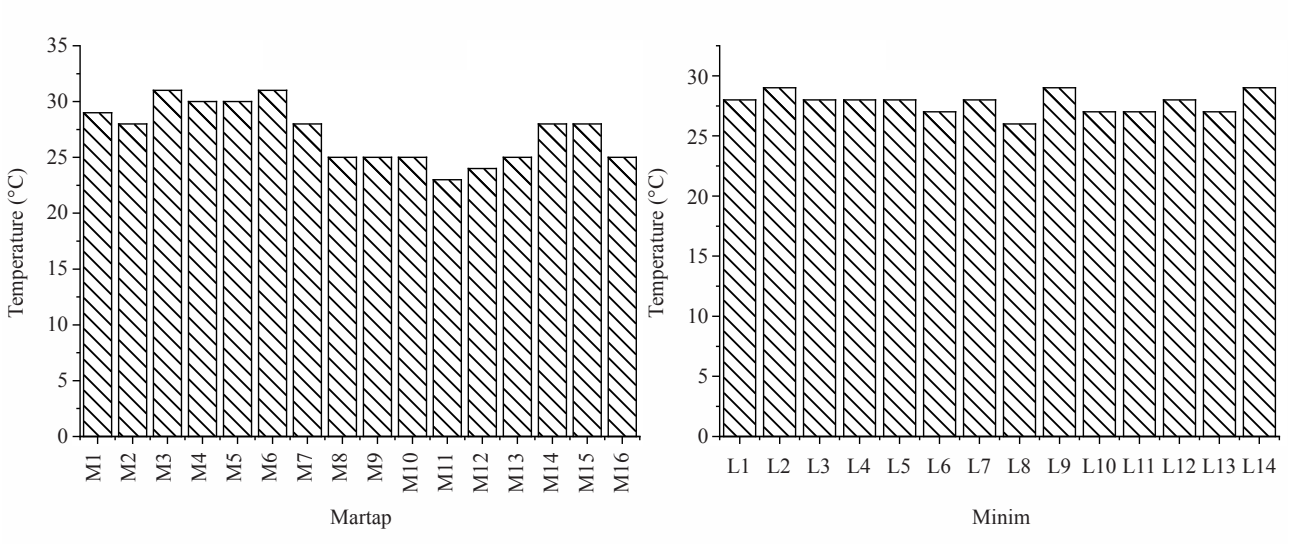

Figure 8. Temperature obtained in the measurement localities

Figures 8 and 9 show that temperature and humidity have acceptable values, according to the World Health Organization (WHO) guidelines on housing and health[50], namely temperatures below 25 °C in the districts of Ngaoundéré 1 and 2 and temperatures range between 25 °C and 30 °C in Martap and Minim. The low temperatures obtained in these localities are one of the peculiarities of the Adamawa region, one of the coldest regions in Cameroon. The measurements were taken in November, the month of the year when it is cold throughout the Adamawa region. This cold climate period generally extends from November to February of the following year.

The second atmospheric parameter, which is the humidity in Figure 9, is very proportional to the temperature. The lower the temperature, the higher the humidity, which explains the high increases in humidity in Ngaoundéré 1 and 2 compared to low and fluctuating values in the cities of Martap and Minim.

Figure 10 presents the distributions of CO_2 concentrations obtained in the four research areas, namely Minim, Martap, Ngaoundéré 1 and 2. Logically, areas with low CO_2 concentrations are in dark green, areas with medium CO_2 concentrations are in light green and yellow, while areas with high CO_2 concentrations are in orange and red, as indicated in the legends of each distribution in Figure 10.

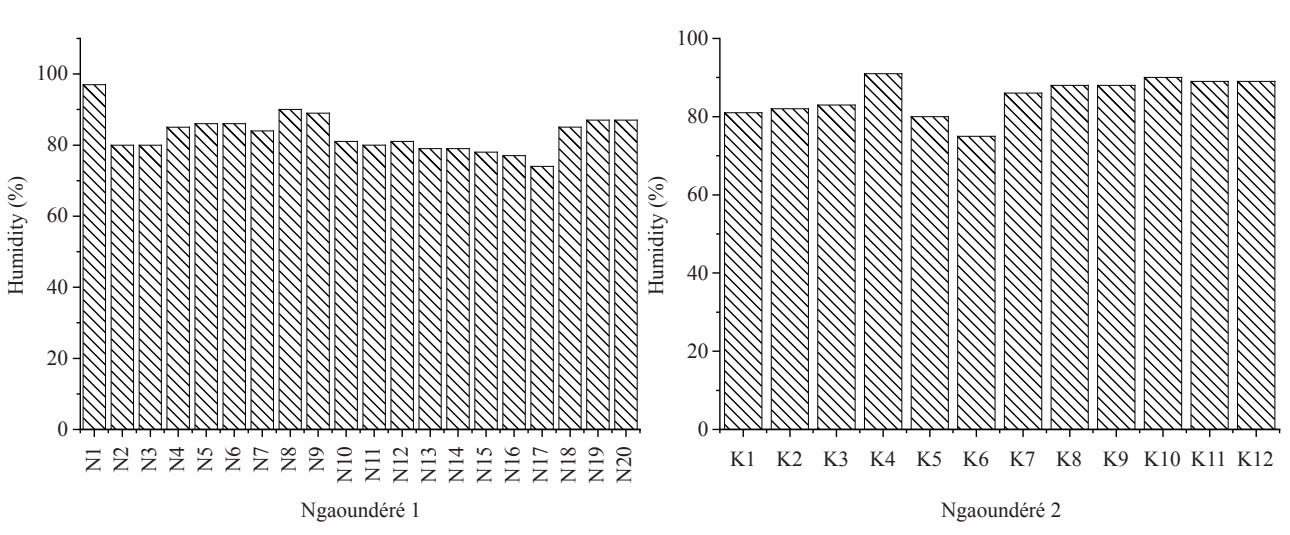

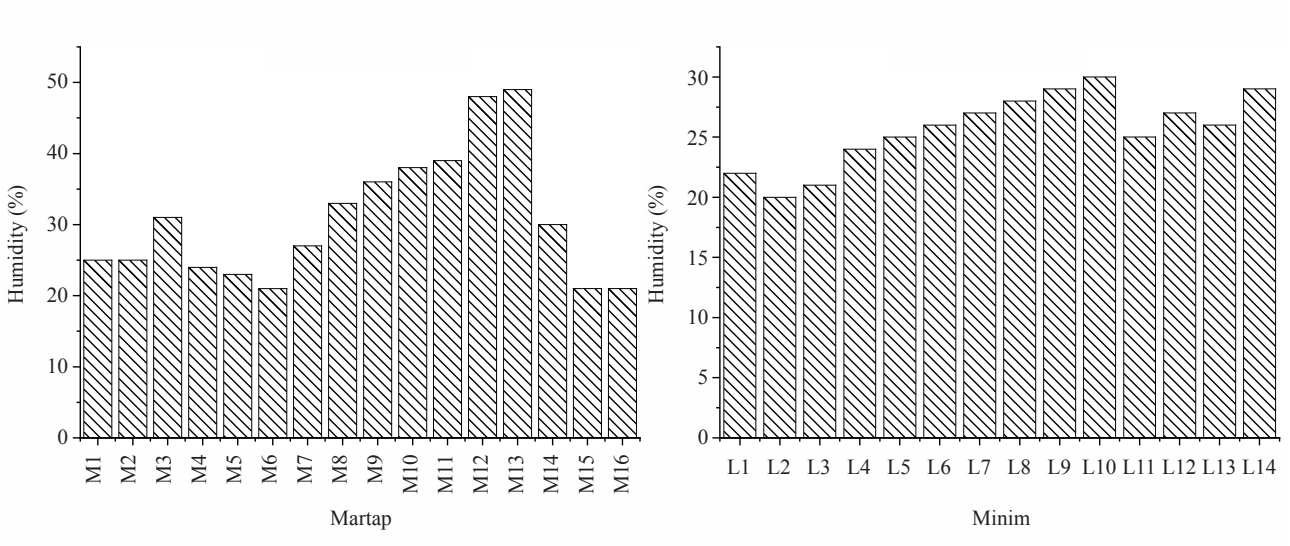

Figure 9. Humidity obtained in the measurement localities

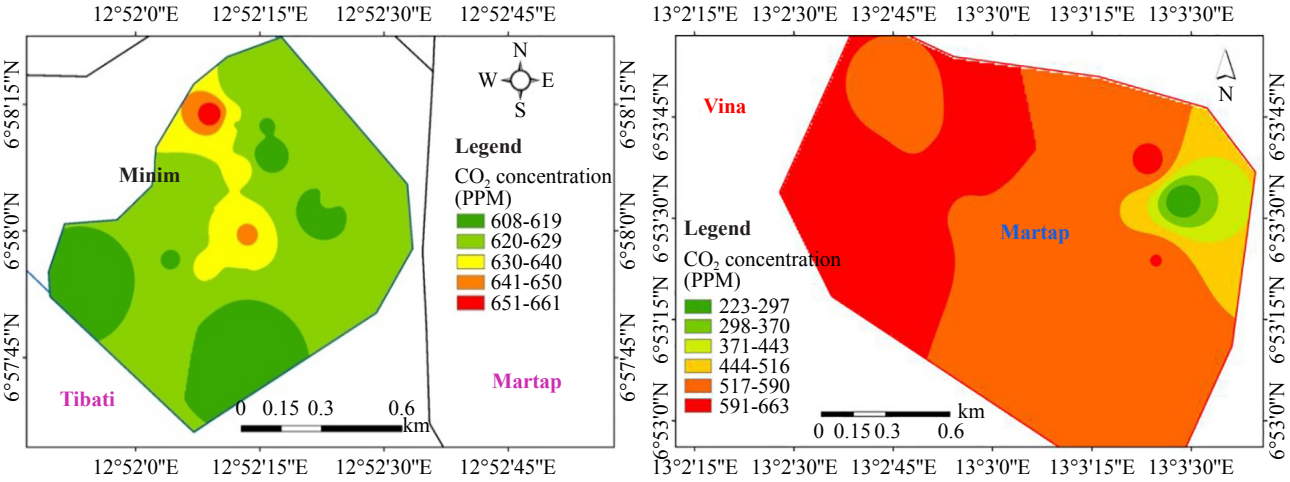

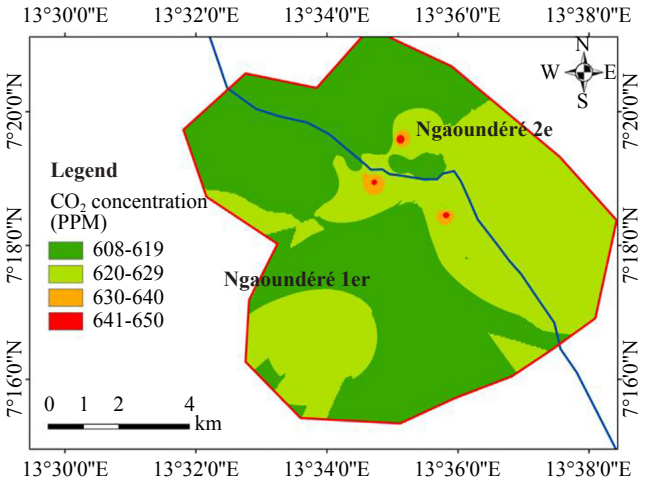

Figure 10. Distribution of CO_2 concentrations obtained in the measurement localities

Figure 10 presents the distributions of CO_2 concentrations obtained in the four research areas, namely Minim, Martap, Ngaoundéré 1 and 2. Logically, areas with low CO_2 concentrations are in dark green, areas with medium CO_2 concentrations are in light green and yellow, while areas with high CO_2 concentrations are in orange and red, as indicated in the legends of each distribution in Figure 10.

Analogous to the distributions of previous CO_2 concentrations, the log-normal distributions of the number of CO_2 measurements taken at each location are shown in Figure 10. Of the 20 measurement points carried out in Ngaoundéré 1 and shown in Figure 11, 3 points have CO_2 concentrations in the range of 400 to 450 ppm, 10 points between 450-500 ppm, 4 between 500-550 ppm, 1 point in the 550-600 ppm range, and 2 between 600-650 ppm. This explains the approximation of the average CO_2 concentration in Ngaoundéré 1 (497.30 ± 11.32 ppm) to the highest values. In Ngaoundéré 2 (Figure 11), all CO_2 concentrations are in the range of 450 to 500 ppm and only one value is 600-650 ppm. The average concentration of this locality is 481.83 ± 14.90 ppm. In Martap (Figure 11), only one concentration is in the range of 200-300 ppm and all others are the 500 to 700 ppm range. The same observation is in Minim (Figure 11) where the concentrations range from 600 to 670 ppm. These last two cities are those with high CO_2 concentrations. This can certainly be explained by the low wind circulation in these two cities during the sampling period, as they are located in the middle of forest and bauxite areas of the Adamawa region.

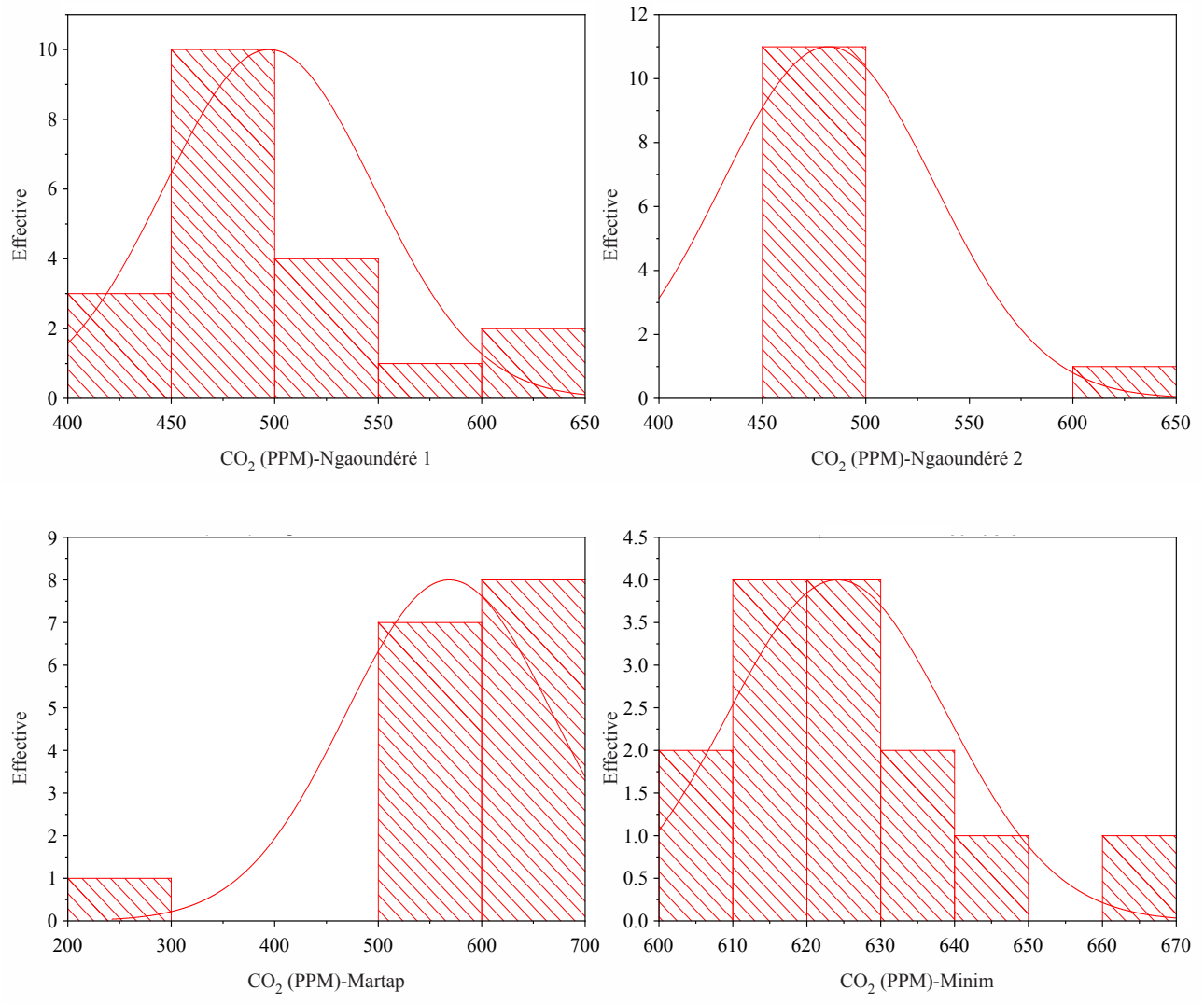

Figure 11. Log-normal distribution of CO_2 concentrations obtained in the measurement localities

A comparative study of the average CO_2 concentrations obtained at the four study sites with reference values such as the normal concentration of atmospheric CO_2 and the average CO_2 measurements from the MLO in November 2022 was performed and presented in Table 5.

Table 5. Comparison of CO_2 concentrations obtained with certain reference values

CO_2 Average concentrations during November 2022 around the world				
measured pollutant	Adamawa Region Cameroon		Mauna Loa Observatory, Hawaii (USA)[51]	Normal atmospheric concentration[45]
CO_2 (ppm)	Ngaoundere 1	497,30 ± 11,32	417.51	400
	Ngaoundere 2	481,83 ± 14,90		
	Martap	568,63 ± 25,028		
	Minim	624,14 ± 3,96		

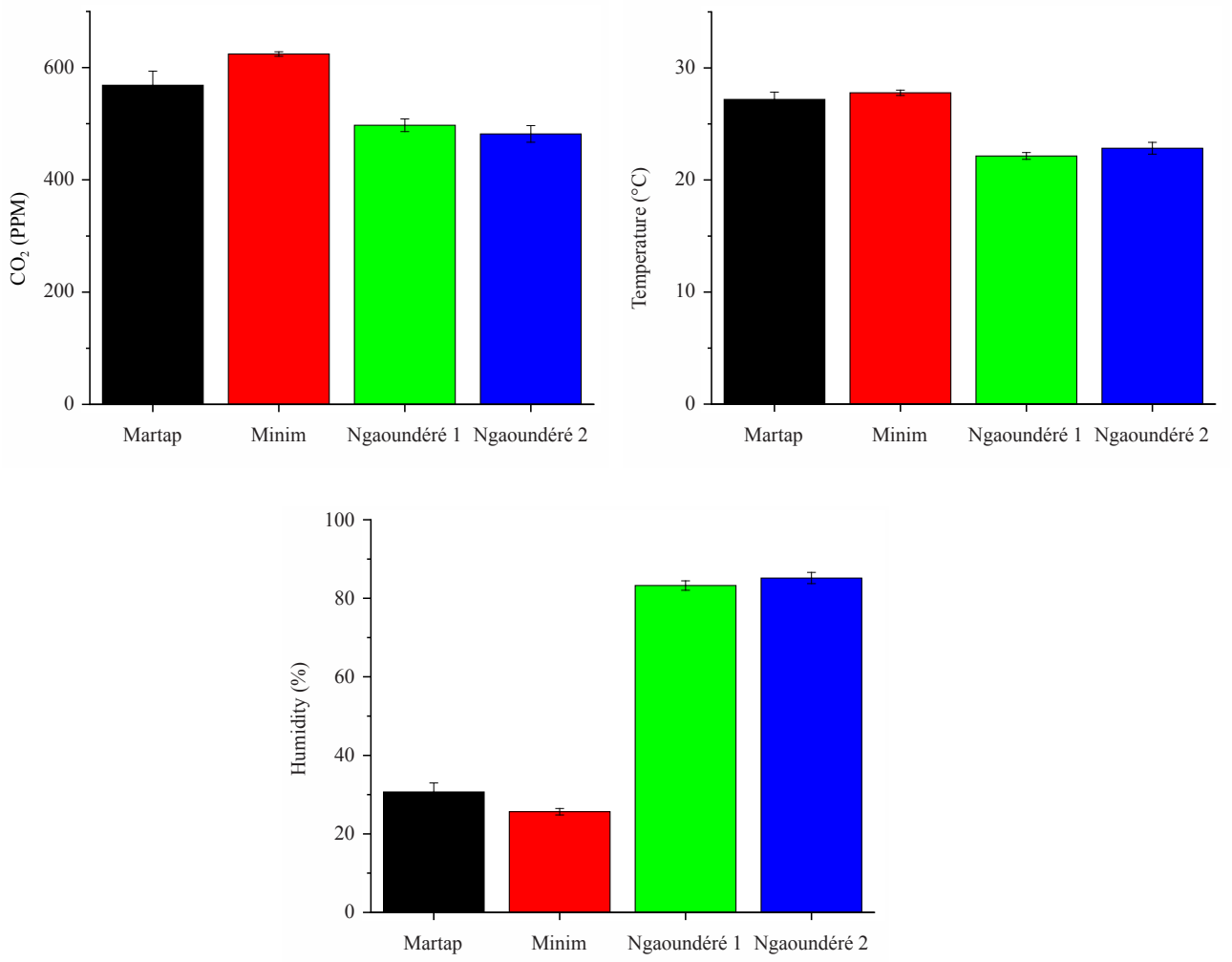

Figure 12. Histograms of average concentrations of measured pollutants

The concentrations obtained in the Adamawa region are well above the reference value. This is explained by the fact that the measurements were taken in public places. These averages in Table 5 made it possible to display the graphs in Figure 12, which are essential for an overall analysis of CO_2 concentrations and measured atmospheric parameters. These plots visually show the distribution of the numerical data and the asymmetry by displaying the average range of the concentrations obtained. They summarize the data set into three elements, namely the minimum score, the average and the maximum score.

3.2 *CO_2-based outdoor air quality assessment*

The aim of this work is to protect people from the harmful effects of air pollution. Therefore, it is then necessary to know the AQI in the four study areas. The following equation (9) makes it possible to determine the different indices based on only CO_2. The results of the obtained AQIs are presented in Table 6. All AQI values obtained are in the range of 51 to 100 and according to Table 6, the corresponding air quality is moderate.

$$\text{AQI} = (\text{Average } CO_2 \text{ concentration}/\text{Atmospheric reference value}) \times 50 \quad (9)$$

This work shows the importance of realizing electronic devices for air quality monitoring, and generally, some devices available on the market, presented in[29,52], are portable, efficient, and measure few gases. Some use short-range Wi-Fi applications for wireless data transmission. However, the device developed in this article measures CO_2 and atmospheric parameters, helps to determine the AQI, and uses XBee S2C 2.4 GHz band radio communication modules that provide wireless data transmission over long distance (more than 1,200 m) to a remote PC via the XCTU enable application. These low-power XBee S2C modules are suitable for dense and mesh equipment networks[53-55]. The special feature of this device is the use of the XBee module, which allows data transfer over long distances without an internet connection. In addition, the device is in the box, autonomous, portable and can be deployed in the field for indoor and outdoor measurements.

Table 6. Air quality index and level of health impact in the study localities [29]

Standard AQI Values	AQI Ngaoundéré I	AQI Ngaoundéré II	AQI Martap	AQI Minim	Levels of Health Concern
From 0 to 50					Good
From 51 to 100	62.16	60.22	71.08	78.02	Moderate

4. Conclusion

This paper presents a real-time CO_2 monitoring device developed and used for air quality sampling. The device uses ZigBee wireless transmission components as an IoT tool. A comparative study of the device carried out with a reference device showed $R^2 = 0.6889$ and the slope test of the regression line according to the Student method showed $t_{(1\%;\ 19)} = 2.539$. The measurement campaign carried out in November 2022 in four subdivisions of the Adamawa region of Cameroon made it possible to obtain average levels of CO_2 equal to 497.30 ± 11.32 ppm with a maximum of 618 ppm and a minimum of 443 ppm in Ngaoundéré 1, 481.83 ± 14.90 ppm with a maximum of 640 ppm and a minimum of 453 ppm in Ngaoundéré 2, 568.63 ± 25.03 ppm with a maximum of 663 ppm and a minimum of 223 ppm in Martap and, 624.14 ± 3.96 ppm with a maximum of 661 ppm and a minimum of 608 ppm in Minim town located in Djérem division. These values indicate a moderate AQI in these cities during the measurement period. The realized equipment has shown that low-cost sensors are of great interest for air quality sampling. They are used for air pollution monitoring in developing countries, where air pollution has adverse effects on human health. Improvement and optimization work is currently being carried out on this realized prototype to obtain a final decision support tool for air pollution.

Funding

This work was supported by the International Atomic Energy Agency (IAEA) through the coordinated research project CRP J02014 and by The Environmental Radioactivity Research Network Center of the University of Tsukuba through the joint research project ERAN Y-23-15, Y-23-17 and I-23-24.

Disclosure statement

No potential conflict of interest was reported by the authors.

Conflict of interest

The authors declare no competing financial interest.

References

[1] Al Katheeri, E.; Al Jallad, F.; Al Omar, M. Assessment of gaseous and particulate pollutants in the ambient air in Al Mirfa City, United Arab Emirates. *J. Environ. Prot*. **2012,** *3*(7), 640-647.
[2] Alam, M.; Khan, M.; Khairulalam, M.; Syed, A.; Rajkumar, R. Azam, TB. Industrial level analysis of air quality and sound limits monitoring in Bangladesh using real time control system. *Vibroengineering Procedia* **2017,** *16*, 81-86.
[3] Chan, C. K.; Yao, X. Air pollution in mega cities in China. *Atmos. Environ*. **2008,** *42*(1), 1-42.
[4] Ashraf, M. A.; Maah, M. J.; Yusoff, I. Soil contamination, risk assessment and remediation. *Environmental Risk Assessment of Soil Contamination* **2014,** *1*, 3-56.
[5] Gougoulias, C.; Clark, J. M.; Shaw, L. The role of soil microbes in the global carbon cycle, tracking the below-ground microbial processing of plant-derived carbon for manipulating carbon dynamics in agricultural systems. *J. Sci. Food Agric*. **2014,** *94*(12), 2362-2371.
[6] Morison, J.; Lawlor, D. J. P. Interactions between increasing CO_2 concentration and temperature on plant growth. *Plant, Cell & Environment* **1999,** *22*(6), 659-682.
[7] Stan, C. *Energy versus carbon dioxide*; Springer, 2022.
[8] Ramanathan, V.; Feng, Y. Air pollution, greenhouse gases and climate change, global and regional perspectives. *Atmos. Environ*. **2009,** *43*(1), 37-50.
[9] Shuangchen, M.; Jin, C.; Kunling. J.; Lan, M.; Sijie, Z.; Kai, W. J. R. Environmental influence and countermeasures for high humidity flue gas discharging from power plants. *Renew. Sustain. Energy Rev*. **2017,** *73*, 225-235.
[10] Hall, A.; Manabe, S. Effect of water vapor feedback on internal and anthropogenic variations of the global hydrologic cycle. *J. Geophys. Res. Atmos*. **2000,** *105*(D5), 6935-6944.
[11] Pierrehumbert, R. T. Subtropical water vapor as a mediator of rapid global climate change. *Geophys. Monogr. Ser.* **1999,** *112*, 339-362.
[12] Chatzidiakou, L.; Mumovic, D.; Summerfield, A. *J. Intell. Build. Int*. **2012,** *4*(4), 228-259.
[13] Stupfel, M. Recent advances in investigations of toxicity of automotive exhaust. *Environ Health Perspect* **1976,** *17*, 253-285.
[14] Pino, H.; Pastor, V.; Grimalt-Álvaro, C.; López, V. *Measuring CO_2 with an Arduino, creating a low-cost, pocket-sized device with flexible applications that yields benefits for students and schools*; ACS Publications, 2018.
[15] Lapshina, P. D.; Kurilova, S. P.; & Belitsky, A. A. *Development of an Arduino-based CO_2 Monitoring Device*; EIConRus, IEEE, 2019; pp 595-597.
[16] Marques, G.; Ferreira, C. R.; Pitarma, R. Indoor air quality assessment using a CO_2 monitoring system based on internet of things. *J. Med. Syst*. **2019,** *43*, 1-10.
[17] Karami, M.; McMorrow, G. V.; Wang, L. Continuous monitoring of indoor environmental quality using an Arduino-based data acquisition system. *J. Build. Eng*. **2018,** *19*, 412-419.
[18] Dari, G. U.; Hamdani, D.; Setiawan, I. Technology. design and build a hazardous gas monitoring device (CO, CO_2,

CH_4) upon cigarette smoke in an enclosed space based on arduino uno and GSM SIM 900 A. *J. Technol. Res*. **2022,** *8*(2), 289-302.
[19] Sadeghi, M.; Esmaeilzadeh, F.; Mowla, D.; Zandifar, A. Technology P. Improving CO_2 capture in UTSA-16 (Zn) via alkali and alkaline earth metal Introduction, GCMC and MD simulations study. *Sep. Purif. Technol.* **2024,** *338*, 126534.
[20] Pereira, P. F.; Ramos, N. M. Low-cost Arduino-based temperature, relative humidity and CO_2 sensors-An assessment of their suitability for indoor built environments. *J. Build. Eng*. **2022,** *60*, 105151.
[21] Moreno, J. R.; Pinna-Hernández, M. G.; Molina, J. S.; Fernández, M. F.; Hernández, J. L.; Fernández, F. A. Carbon capture from biomass flue gases for CO_2 enrichment in greenhouses. *Heliyon*. **2024,** *10*(1), e23274.
[22] Ellis, E. C. *Anthropocene, a very short introduction*; OUP, 2018.
[23] Kleypas, J. A.; Feely, R. A.; Fabry, V. J.; Langdon, C.; Sabine, C. L.; Robbins, L. L. Impacts of ocean acidification on coral reefs and other marine calcifiers, a guide for future research. *Report of a Workshop Held* **2005,** *18*, 20.
[24] Johansen, B. E. Science, Why so urgent? Saving ourselves from ourselves. *Global Warming and the Climate Crisis, Science, Spirit, and Solutions*; Springer, 2023; pp 17-96.
[25] Colls, J.; Tiwary, A. *Air pollution, measurement, modelling and mitigation*; CRC Press, 2017.
[26] Cooper, C. D.; Alley, F. C. *Air pollution control, A design approach*; Waveland press, 2010.
[27] Metwally, I. A. Failures, monitoring and new trends of power transformers. *IEEE Potentials* **2011,** *30*, 36-43.
[28] Schneider, S. H. J. S. A. The changing climate. *Scientific American Magazine* **1989,** *261*(3), 70-79.
[29] Jacob, M. T.; Nasser, N.; Michaux, K. N.; Flore, Y.; Siaka, T. Zigbee-based wireless smart device for enclosed space real-time air quality monitoring, experiment, data analysis and risk assessment. *Indoor Air Quality Assessment for Smart Environments*; IOS Press, 2022; pp 55.
[30] Jenkin, M. E.; Clemitshaw, K. C. Ozone and other secondary photochemical pollutants, chemical processes governing their formation in the planetary boundary layer. *Atmos. Environ*. **2000,** *34*, 2499-527.
[31] Kambire, P. S.; Auti, A. S.; Barge, A. A.; Badadapure, P. R. *Drone Delivery System*; IRJET, 2019.
[32] Kao, A. S. Formation and removal reactions of hazardous air pollutants. *Air & Waste* **1994,** *44*, 683-696.
[33] Katz, M. Advances in the analysis of air contaminants, a critical review. *J. Air Pollut. Control Assoc*. **1980,** *30*(5), 983-997.
[34] Kuhn, D. M.; Ghannoum, M. Indoor mold, toxigenic fungi, and Stachybotrys chartarum, infectious disease perspective. *Clin Microbiol Rev*. **2003,** *16*(1), 144-72.
[35] Buermann, W.; Lintner, B. R.; Koven, C. D.; Angert, A.; Pinzon, J. E.; Tucker, C. J.; Fung, I. Y. The changing carbon cycle at Mauna Loa Observatory. *Proceedings of the National Academy of Sciences of the United States of America* **2007,** *104*(11), 4249-4254.
[36] Elliott, W. P.; Machta, L.; Keeling, C. D. An estimate of the biotic contribution to the atmospheric CO_2 increase based on direct measurements at Mauna Loa Observatory. *J. Geophys. Res. Atmos*. **1985,** *90*, 3741-3746.
[37] Vehviläinen, T.; Lindholm, H.; Rintamäki, H.; Pääkkönen, R.; Hirvonen, A.; Niemi, O.; Vinha, J. High indoor CO_2 concentrations in an office environment increases the transcutaneous CO_2 level and sleepiness during cognitive work. *J. Occup. Environ. Hyg*. **2016,** *13*(1), 19-29.
[38] Becerra, J. A.; Lizana, J.; Gil, M.; Barrios-Padura, A.; Blondeau, P.; Chacartegui, R. Identification of potential indoor air pollutants in schools. *J. Clean. Prod*. **2020,** *242*, 118420.
[39] Brändle, J.; Kunert, N. A new automated stem CO_2 efflux chamber based on industrial ultra-low-cost sensors. *Tree Physiol*. **2019,** *39*(12), 1975-1983.
[40] Yang, S.; Huang, Z.; Wang, C.; Ran, X.; Feng, C.; Chen, B. A real-time occupancy detection system for unoccupied, normally and abnormally occupied situation discrimination via sensor array and cloud platform in indoor environment. *Sensors and Actuators A, Physical* **2021,** *332*, 113116.
[41] Finlayson, G. D.; Drew, M. S. Constrained least-squares regression in color spaces. *J. Electron. Imaging* **1997,** *6*(4), 484-493.
[42] Andrade, J. M.; Estévez-Pérez, M. G. Statistical comparison of the slopes of two regression lines, A tutorial. *Anal. Chim. Acta*. **2014,** *838*, 1-12.
[43] Strømsø, H. I.; Bråten, I.; Samuelstuen, M. S. Students' strategic use of multiple sources during expository text reading, A longitudinal think-aloud study. *Cognition and Instruction*. **2003,** *21*(2), 113-147.
[44] Taillefer, G. Reading for academic purposes, The literacy practices of British, French and Spanish law and economics students as background for study abroad. *J. Res. Read*. **2005,** *28*(4), 435-451.
[45] Satish, U.; Mendell, M. J.; Shekhar, K.; Hotchi, T.; Sullivan, D.; Streufert, S.; Fisk, W. J. Is CO_2 an indoor pollutant? Direct effects of low-to-moderate CO2 concentrations on human decision-making performance. *Environ Health Perspect* **2012,** *120*(12), 1671-1677.

[46] Bierwirth, P. N. Carbon dioxide toxicity and climate change, a major unapprehended risk for human health. *Research Gate*. **2018,** *10*, 1-18.
[47] Pörtner, H. O.; Langenbuch, M.; Michaelidis, B. Synergistic effects of temperature extremes, hypoxia, and increases in CO_2 on marine animals, from earth history to global change. *J. Geophys. Res. Oceans*. **2005,** *110*(C9).
[48] Krishnan, P.; Swain, D. K.; Bhaskar, B. C.; Nayak, S. K.; Dash, R. N. ecosystems, environment. Impact of elevated CO_2 and temperature on rice yield and methods of adaptation as evaluated by crop simulation studies. *Agric. Ecosyst. Environ*. **2007,** *122*(2), 233-242.
[49] Mendell, M. J.; Eliseeva, E. A.; Davies, M. M.; Spears, M.; Lobscheid, A.; Fisk, W. J.; Apte, M. G. Association of classroom ventilation with reduced illness absence, A prospective study in C alifornia elementary schools. *Indoor Air*. **2013,** *23*(6), 515-528.
[50] World Health Organization. *WHO housing and health guidelines*; World Health Organization; 2018.
[51] Price, S.; Pales, J. Mauna Loa Observatory, the first five years. *Monthly Weather Review* **1963,** *91*, 665-680.
[52] Smith, K. R. National burden of disease in India from indoor air pollution. *Proceedings of the National Academy of Sciences of the United States of America*. **2000,** *97*(24), 13286-13293.
[53] Smith, K. R.; Mehta, S. The burden of disease from indoor air pollution in developing countries, comparison of estimates. *J. Hyg. Environ Health* **2003,** *206*(4-5), 279-289.
[54] Thunis, P.; Miranda, A.; Baldasano, J. M.; Blond, N.; Douros, J.; Graff, A.; White, L. Overview of current regional and local scale air quality modelling practices, Assessment and planning tools in the EU. *Environ Sci Policy*. **2016,** *65*, 13-21.
[55] Trasviña-Moreno, C. A.; Blasco, R.; Marco, Á.; Casas, R.; Trasviña-Castro, A. Unmanned aerial vehicle based wireless sensor network for marine-coastal environment monitoring. *Sensors*. **2017,** *17*(3), 460.

Appendix

Device operation algorithm

```
Loop
// MH-Z14A CO2 Sensor //
char getCheckSum(char *packet) {
char i, checksum;
for (i = 1; i < 8; i++) {
 checksum += packet[i]; }
 checksum = 0xff-checksum;
 checksum += 1;
   return checksum; }
End if
// AMT1001, T and RH Sensor //
Begin
uint16_t step = analogRead(tempPin);
float temperature = amt1001_gettemperature(step);
return temperature ;
uint16_t step1 = analogRead(humPin);
double volt = (double)step1 * (5.0/1023.0);
humidity = amt1001_gethumidity(volt);
return humidity;
End
End loop
```